Journal Pre-proof

A Simple, One-pot and Ultrasensitive DNA Sensor via Exo III-Assisted Target Recycling and 3D DNA Walker Cascade Amplification

Na Wu, Yi-Ting Wang, Xiao-Yan Wang, Xu- Wei Chen, Ting Yang, Jian-Hua Wang

PII: S0003-2670(20)31219-8

DOI: https://doi.org/10.1016/j.aca.2020.12.026

Reference: ACA 238151

To appear in: *Analytica Chimica Acta*

Received Date: 12 October 2020

Revised Date: 13 December 2020

Accepted Date: 15 December 2020

Please cite this article as: N. Wu, Y.-T. Wang, X.-Y. Wang, X.-.W. Chen, T. Yang, J.-H. Wang, A Simple, One-pot and Ultrasensitive DNA Sensor via Exo III-Assisted Target Recycling and 3D DNA Walker Cascade Amplification, *Analytica Chimica Acta*, https://doi.org/10.1016/j.aca.2020.12.026.

Credit author statement

- **Na Wu:** Writing- Original draft preparation
- **Yi-Ting Wang:** Data curation
- **Xiao-Yan Wang:** Data curation
- **Xu- Wei Chen:** Supervision
- **Ting Yang:** Writing- Reviewing and Editing, Supervision
- **Jian-Hua Wang:** Conceptualization, Methodology

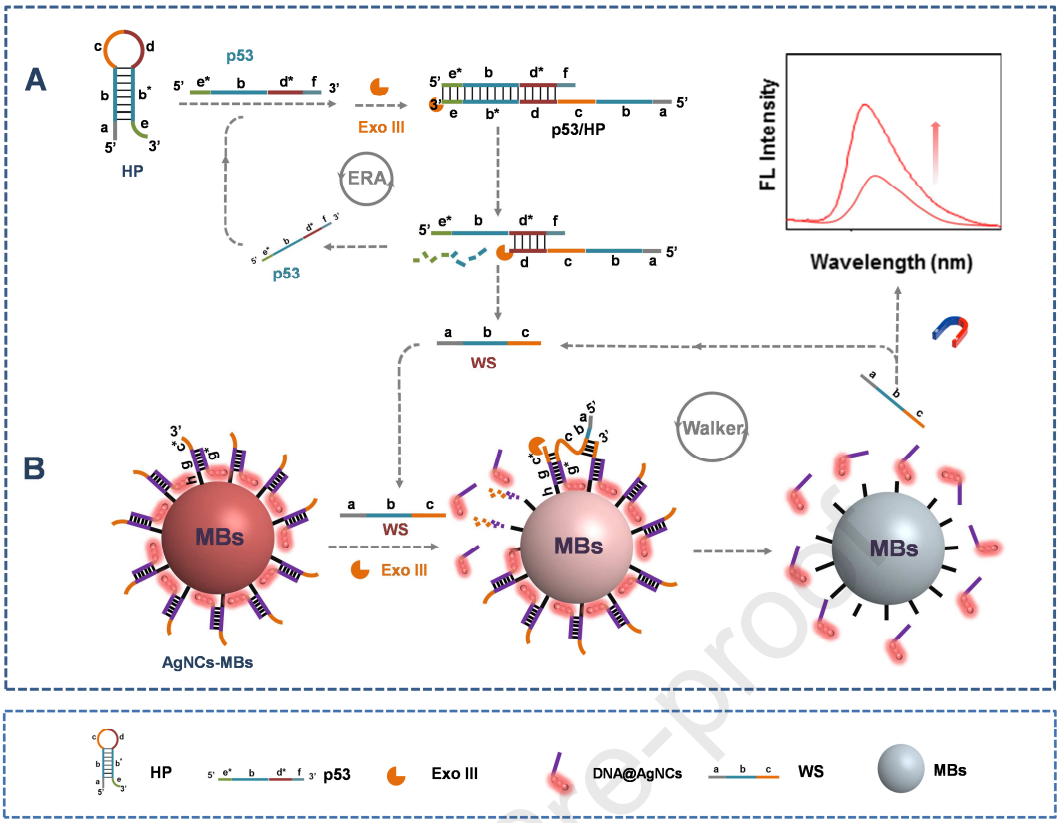

A Simple, One-pot and Ultrasensitive DNA Sensor via Exo III-Assisted Target Recycling and 3D DNA Walker Cascade Amplification

Na Wu, Yi-Ting Wang, Xiao-Yan Wang, Xu- Wei Chen, Ting Yang*, Jian-Hua Wang

Research Center for Analytical Sciences, Department of Chemistry, College of Sciences, Northeastern University, Box 332, Shenyang 110819, China

*E-mail: yangting@mail.neu.edu.cn (T. Yang).

Corresponding author.
Phone: +86 24 83688944 Fax: +86 24 83676698 E-mail: yangting@mail.neu.edu.cn (T. Yang).

Abstract

Rapid, sensitive, and user-friendly nucleic acid detection is of growing importance in early clinical diagnosis. Here, we construct a simple, one-pot and ultrasensitive DNA sensor via exonuclease III (Exo III)-assisted target recycling amplification (ERA) combined with 3D DNA walker cascade amplification. In the presence of single-stranded DNA target, the ERA process is activated to generate numerous walker strands (WS). Thereafter, Exo III-powered WSs autonomously move along magnetic bead (MB)-based 3D track to release numerous AgNCs into the supernatant as an amplified signal output. This biosensor had a low detection limit of 18 fM and an analytical range of 40 fM to 1 pM. Furthermore, the practical application potential of this biosensor was also confirmed by the spiking experiments of p53 into human serum and urine samples.

Keywords: One-pot; Exo III-assisted target recycling; 3D DNA walker; amplification;

1. Introduction

Cancer is a great threat to human health [1]. Nowadays, early cancer diagnosis through the detection of tumor-related biomarker, including cancer-related genes, miRNA, etc., is a promising way to improve the survival rate of cancer patients [1,2]. However, the low abundance of these biomarkers brings great challenge to early cancer diagnosis. Therefore, it is necessary to develop accurate and ultrasensitive detection approaches for cancer-related DNA [3]. Nucleic acids are widely used in the detection of cancer-related DNA due to their excellent programming ability and accurate base recognition property [4-7]. As a gold standard approach for amplifying and detecting nucleic acids at low levels, polymerase chain reaction (PCR) requires large and expensive thermal cyclers, which largely limit the application of PCR in resource-limited settings and for point-of-care (POC) analysis [4,8,10,15]. In the past decades, isothermal amplification of nucleic acid has emerged in the field of biological detection [4,6,12]. However, single step amplification is limited by low signal gain and assay sensitivity [6,16]. To overcome these limitations, techniques integrating two or more amplification methods have been developed [17-21]. The key requirement for cascade amplification is that the product of the first step of amplification can trigger the amplification reaction of the second step. The two steps can therefore be connected and sequentially proceed [4,6]. For instance, Willner et al. designed a cascade amplification strategy based on RCA (rolling circle amplification)/DNAzyme in which a long DNAzyme chain was synthesized in the first step to perform a second amplification reaction [11].So far, various isothermal

cascade amplification strategies have been constructed and applied to biosensing [22-29]. Isothermal cascade amplifications can be roughly divided into enzymatic and enzyme-free amplification [6]. Enzyme-free isothermal cascade amplification strategies offer advantages of high stability and low cost, and are therefore particularly attractive for *in vivo* applications [14]. However, enzyme-free strategies suffer from long reaction cycle and non-specific binding [15]. Enzyme-assisted cascade amplification shows high amplification efficiency and hybridization specificity [10,11,16]. While, some of the enzymes, such as DNase-I enzyme and DNAzymes, are sequence-dependent, thus requiring sophisticated design, which largely restricts their applications [10,18]. On the contrary, exonuclease III (Exo III) is a sequence-independent enzyme, and can be easily utilized without the consideration of specific enzymatic recognition sites [18-20]. The Exo III-assisted target recycling amplification (ERA) emerges as a powerful isothermal nucleic acid amplification technique and has attracted wide attention due to its simple operations and high amplification efficiency [21-23].

To maximize the sensitivity of biosensors, nucleic acid functionalized nanomaterials were introduced into the nucleic acid amplification systems [24-29]. The large surface area of nanomaterials can significantly improve the loading efficiency of DNA thus improving the amplification capability. A typical example is three-dimensional (3D) DNA walker, which is constructed on the surface of nanoparticles and shows higher walking efficiency and better signal amplification capability compared with its one-dimensional or two-dimensional counterparts

[27-30]. Generally, DNA walker is mainly composed of three parts, namely the driving force, the walking track, and the walking strand [26]. The driving force activates the DNA walker in the form of energy conversion. When the driving force breaks the initial balance, it can convert the light energy or chemical energy into mechanical energy, propelling the walking strand to walk along the walking track. [26]. Then, through the consumption of fuel molecules, the reaction balance is restored by consuming fuel materials, sequentially generating a signal [26]. The reaction balance is constantly broken and restored, and finally generates an amplified output [26]. Due to the excellent signal amplification ability, DNA walkers have attracted extensive attention in biosensing in the past decades [26]. Our research group has recently designed a cascade amplification strategy based on ERA and DNA walker with relatively simple DNA design and high sensitivity [29]. However, DNA walker in that system was powered by chain replacement, which potentially prolonged the reaction time, limited the reaction rate, and increased the probability of non-specific hybridization.

Herein, a one-pot, ultrasensitive DNA sensor was constructed on the combination of the Exo III-assisted target recycling (ERA) with 3D DNA walker as a novel cascade amplification strategy. In this system, hairpin DNA (HP) hybridizes with the target DNA in the first step of amplification, followed by the digestion of Exo III to release the target. The target hybridizes with another HP, which triggers the Exo III-assisted target recycling amplification (ERA) and produces massive walking strands (WS). Thereafter, powered by Exo III, WS walks on the surface of AgNCs

conjugated-magnetic beads (AgNCs-MBs) and releases AgNCs for fluorescent measurement. In contrast to our previous design, as both amplification steps are powered by Exo III, the two steps are integrated into an one-pot cascade amplification reaction, which simplifies the operation while maintains efficient cleavage. Meanwhile, instead of using fluorophore labeled DNA strands, fluorescent AgNCs prepared by using DNA strands as template are used as the signal probe, facilitating sensitive detection without expensive fluorophore labeling.

2. Experimental Section

2.1 Reagents and materials

All the oligonucleotides were synthesized by Sangon Biotechnology Co., Ltd. (Shanghai, China) and their sequences are listed in Table S1. DNA was prepared by dissolving in 50 mM Tris-HCl buffer (containing 6 mM $MgCl_2$, 10 mM KCl) at pH 8.0 and stored at - 20 °C. The 200 nm- magnetic beads (MBs) were purchased from Sangon Biotechnology Co., Ltd. (Shanghai, China). Exo III, loading buffer and 4S red plus nucleic acid gel stain were purchased from TaKaRa Biotechnology Co., Ltd. (Dalian, China). 1-Ethyl-3-[3-(dimethylamino)-propyl] carbodiimide hydrochloride (EDC) and N-hydroxysuccinimide (NHS) were purchased from Aladdin Chemical Reagent Co., Ltd. (Shanghai, China). Silver nitrate ($AgNO_3$) and sodium borohydride ($NaBH_4$) were obtained from Sigma-Aldrich (St. Louis, Mo, USA). Other chemicals used were analytical reagent grade and obtained from Aladin (Shanghai, China). All aqueous solutions were prepared using deionized (DI) water with a resistivity of 18.2 $M\Omega\ cm^{-1}$ from a Millipore system.

2.2 Apparatus.

The size and morphology of MBs were observed by a field-emission scanning electron microscope (SEM, SSX-550, Shimadzu, Japan). Fluorescence spectra of AgNCs were recorded on an F-7000 fluorescence spectrophotometer (Hitachi High Technologies, Japan) at excitation wavelength of 528 nm. Fluorescence images were observed using an FV1200 confocal fluorescence microscope (Olympus, Japan).

2.3 Preparation of DNA@AgNCs.

AgNCs were prepared according to previously reported protocol [31]. Briefly, 100 μL $DNA_{(AgNCs)}$ (the DNA strands used as the template for AgNCs growth, 10 μM) was mixed with 20 μL $AgNO_3$ (600 μM) and incubated in ice-water bath for 60 min. Then, 20 μL freshly-prepared $NaBH_4$ (600 μM) was added into the above mixture with vigorous shaking for 2 min. The reaction solution was incubated in the dark at 4 °C for 6 h to produce DNA@AgNCs.

2.4 Preparation of AgNCs conjugated - MBs (AgNCs-MBs).

NH_2-terminated anchor strand (AS) was coupled to carboxyl magnetic bead (COOH-MBs) by a one-step carbodiimide reaction. Briefly, 1 mL COOH-MBs (5 mg mL^{-1}) was washed and resuspended in 1 mL MES buffer (100 mM, pH 5.0), followed by the reaction with 200 μL EDC (1 mg mL^{-1}) and 200 μL NHS (1 mg mL^{-1}) for 30 min at room temperature. Then, the activated MBs were repeatedly washed and resuspended in 1 mL TE buffer (10 mM Tris, 10 mM $MgCl_2$, 0.1% tween-20 pH 7.4). 100 μL NH_2-teminated AS strands (7 μM) were added into the activated MBs solution and incubated overnight at room temperature. After incubation, the AS -conjugated MBs (AS-MBs) were suspended in TE buffer (10 mM Tris, 10 mM $MgCl_2$, 0.05% BSA, 0.1% tween-20, pH 7.4) for 60 min to block the non-specific binding sites and then resuspended in 1 mL TE buffer. Afterwards, 100 μL DNA@AgNCs were added

to hybridize with AS-MBs at 37 °C for 14 h. Finally, the excessive DNA@AgNCs was removed by magnetic separation. The resulting AgNCs-MBs were washed with 200 μL TE buffer (pH 7.4) for three times and resuspended in 500 μL of the same buffer and stored at 4 °C for further use. As revealed by SEM analysis (Figure S1A), the diameter of the resulting AgNCs-MBs does not change much (~200 nm). The presence of silver element was confirmed by EDS results (Figure S1B). The fluorescence property of AgNCs-MBs was characterized by confocal fluorescence microscope and fluorescence spectrophotometer with both excitation and emission slits of 10 nm and voltage of 700 V. The fluorescence was detected at $\lambda_{ex}/\lambda_{em}$=528/641 nm.

2.5 Exo III-assisted target cascade amplification.

First, 20 μL hairpin DNA (HP, 1μM), 40 μL AgNCs-MBs, 10 μL Exo III (9 U/100 μL) were mixed with 20 μL p53 with various concentrations. The reaction solution was incubated at 37 °C with gentle shaking at 110 rpm for 70 min. Thereafter, the reaction was stopped by heating at 70 °C for 20 min. After magnetic separation, the supernatant was monitored at 641 nm by a Hitachi F-7000 fluorescence spectrometer.

2.6 PAGE gel electrophoresis.

Non-denaturating polyacrylamide gel electrophoresis (PAGE) was performed to confirm the feasibility of the cascade amplification strategy. The samples were obtained by mixing 10 μL DNA sample (2 μM) and 2 μL loading buffer. The mixture was added into 15% polyacrylamide gel. Next, electrophoresis was run at a constant voltage of 100 V for 45 min in 1× TBE buffer followed by staining with 4S Red Plus for 30 min. Gel images were obtained by an UV digital imaging system (Shanghai

Furi Science & Technology Co. Ltd.)

2.7 Real sample analysis.

Peripheral venous blood samples were obtained from the school hospital of Northeastern University (Shenyang, China), and allowed to clot at 4℃ for 1 h. After centrifuged at 3000 rpm for 10 min, the serum was separated and diluted for 10-fold by Tris-HCl buffer (pH 7.4). Fresh urine samples were provided by healthy volunteers and centrifuged at 8000 rpm for 10 min to remove impurities including crystals, cells, and cell fragments. The supernatant was then diluted for 10-fold by Tris-HCl (pH 7.4) before analysis.

3. Results and discussion

3.1 Principle of the cascade amplification strategy.

The principle of the novel cascade amplification strategy is shown in Scheme 1. First, hairpin DNA (HP) hybridizes with the target DNA and opens up the stem-loop of hairpin structure. As the hybridization generates a blunt end, which is soon recognized by Exo III, the digestion from the 3' end of HP strand begins.0In this way, the Exo III-assisted target recycling amplification (ERA) starts, and large amount of walker strands (WS) are generated for the following DNA walker process. In the second step, the anchor strands (AS) conjugated on MBs' surface are designed to be complementary with AgNCs labeled DNA at g region to form AgNCs-MBs hybridization complex, and the c* part of AS is designed to hybridize with WS. As the ERA proceeds, WS is generated and soon hybridizes with AS to form a recessed 3' end. As Exo III can also recognize the recessed 3' terminus of double-stranded DNA, the cleavage of AS strand from the 3' terminus is triggered. As the cleavage proceeds, WS strand is partially released and the free part of WS hybridizes stochastically with

the proximate AS strand on MBs surface. In this way, the WS walks along the surface of MBs and releases AgNCs into the supernatant. Then, the fluorescence of the supernatant is recorded for quantification.

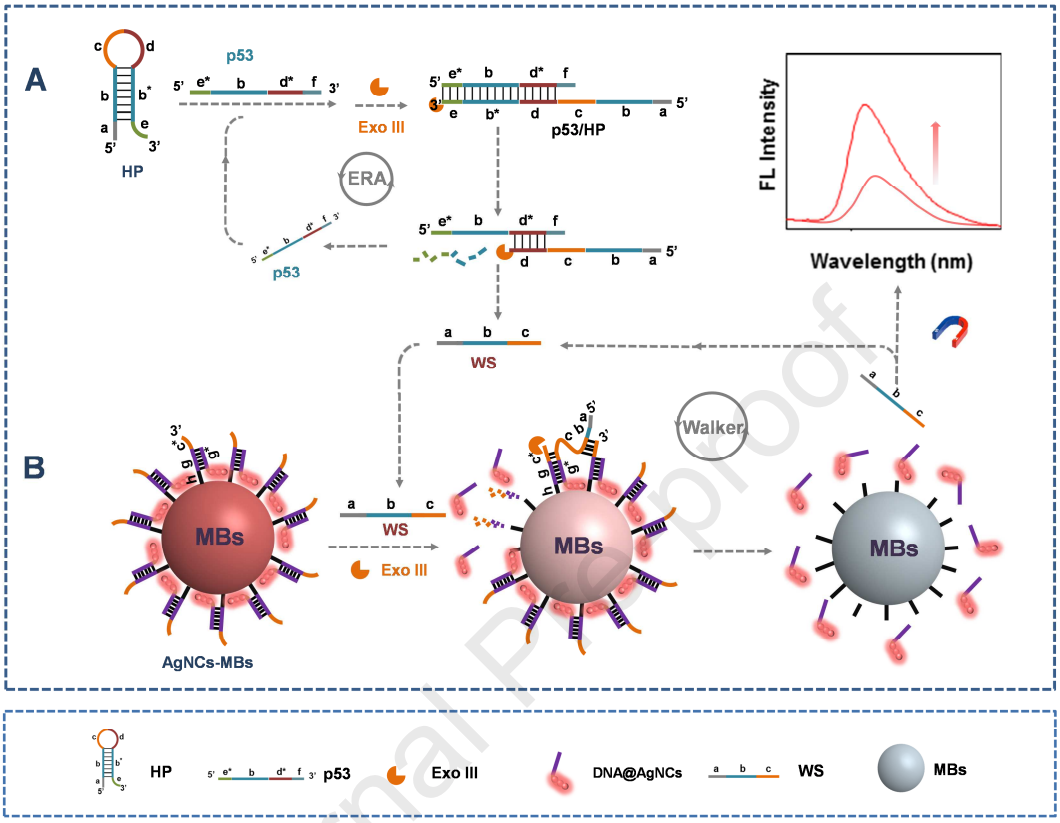

Scheme 1. Schematic illustration of the one-pot cascade amplification strategy for DNA sensing. The amplification strategy is developed by the combination of ERA and 3D DNA walker, where the fluorescence of AgNCs is used as signal output.

3.2 Feasibility of cascade amplification strategy.

The non-denaturating polyacrylamide gel electrophoresis (PAGE) experiment was performed to investigate whether the ERA and walking process could proceed only in the presence of the target. As shown in Figure 1a, when HP is mixed with the target (the p53 DNA), a new band can be observed in lane 5 (p53+HP), indicating the successful hybridization between p53 DNA (lane 1) and HP (lane 2) to form the p53/HP duplex. In lane 6 (p53+HP+Exo III), when Exo III is added to the (p53 + HP) mixture, the band of p53/HP duplex disappears, indicating that Exo III could effectively digest p53/HP duplex to generate walker strands (WS). Meanwhile, it was

observed that $DNA_{(AgNCs)}$ (lane 3) could hybridize with AS (lane 4), which was confirmed by the appearance of a new band in lane 7 ($DNA_{(AgNCs)}$ +AS). When Exo III is added in lane 8 ($DNA_{(AgNCs)}$ +AS+Exo III), the bands are almost the same as that in lane 7, indicating that the AgNCs-AS duplex cannot be digested by Exo III. In lane 9 (p53+HP+ $DNA_{(AgNCs)}$ +AS), the hybridization products of both (p53+ HP) and ($DNA_{(AgNCs)}$ +AS) are observed. In lane 10 (p53+HP+ $DNA_{(AgNCs)}$+AS+Exo III), in the presence of Exo III, the hybridization band of p53/HP and that of AgNCs-AS duplex become shallower, whereas the bands of p53 and $DNA_{(AgNCs)}$ appear. The results herein demonstrated the feasibility of the amplification cascade by combing ERA with 3D DNA walker for target DNA detection. We further tested the feasibility of this biosensing system by comparing the fluorescence response of a series of samples with different components. As shown in Figure 1b, the control groups of A (AgNCs-MBs+Exo III), B (AgNCs-MBs+p53+HP), C (AgNCs-MBs+p53+Exo III) and D (AgNCs-MBs+HP+Exo III) exhibit weak fluorescence intensity. In column E (AgNCs-MBs+HP+p53+Exo III), when all the elements of this biosensor system are present, a strong fluorescence intensity is observed. This indicates that the cascade amplification strategy produces remarkably amplified signal for the detection of target DNA. Moreover, confocal fluorescent microscope images (CLSM) also evidenced the feasibility of this system. As shown in Figure S2A-B, there is no fluorescence emission in the CLSM image when the solution only contains COOH-MBs, whereas red emission is observed when the DNA@AgNCs are successfully loaded on the surface of MBs. Furthermore, upon the addition of p53 and Exo III, the ERA and DNA walker cascade amplification process proceeds, releasing AgNCs into the supernatant. Therefore, as can be seen in Figure 1c, the fluorescence becomes weaker and weaker as the amplification reaction proceeds for 20, 40, 60 min, confirming the

feasibility of this strategy.

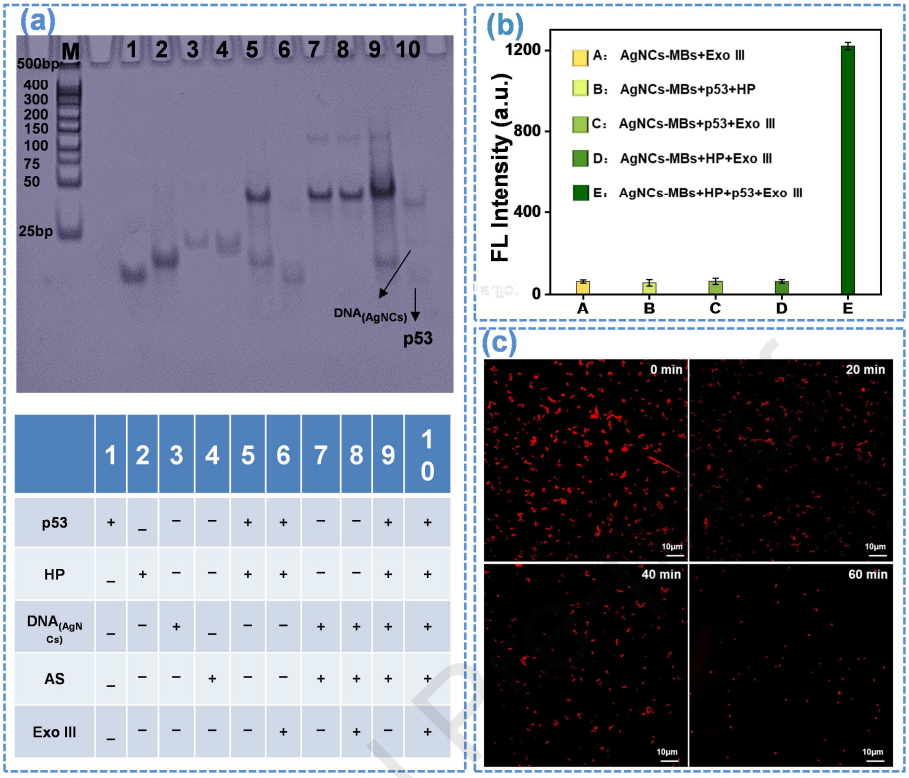

	1	2	3	4	5	6	7	8	9	10
p53	+	_	–	–	+	+	–	–	+	+
HP	_	+	–	–	+	+	–	–	+	+
$DNA_{(AgNCs)}$	_	–	+	_	–	–	+	+	+	+
AS	_	–	–	+	–	–	+	+	+	+
Exo III	_	–	–	–	–	+	–	+	–	+

Figure 1. Characterization of cascade amplification of the one-pot cascade amplification system. (a) PAGE (15%) images. All reactions were run at 30 °C for 45 min. The concentration of each standard DNA sample was set as 2 μmol L^{-1}. Lanes: (1) p53, (2) HP, (3) $DNA_{(AgNCs)}$, (4) AS, (5) mixture of p53 and HP, (6) mixture of HP, p53 and Exo III, (7) mixture of AS and $DNA_{(AgNCs)}$, (8) mixture of AS, $DNA_{(AgNCs)}$ and Exo III, (9) mixture of HP, p53, AS and $DNA_{(AgNCs)}$, and (10) mixture of HP, p53, AS, $DNA_{(AgNCs)}$ and Exo III. (b) Fluorescence intensity of this biosensor at different experimental conditions: (A) AgNCs-MBs+Exo III, (B) AgNCs-MBs+p53+HP, (C) AgNCs-MBs+p53+Exo III, (D) AgNCs-MBs+HP+Exo III, (E) AgNCs-MBs+p53+HP+Exo III. The concentration of p53 was 1 pM. The fluorescence intensity was recorded at $\lambda_{ex}/\lambda_{em}$ =528 nm /641 nm. Error bars indicate the standard deviation of triplicated test. (c) Confocal fluorescent microscope images (CLSM) of AgNCs-MBs reacting with Exo III, p53 and HP for 0 min, 20 min, 40 min, 60 min. Experimental conditions for (c): Exo III: 9 U/100 μL, 10 μL; p53: 500 fM, 20 μL; HP: 20 μL, AgNCs-MBs: 40 μL, reacting at 37 °C for different times and terminated by 70 °C-heating for 20 min.

3.3 Optimization of experimental conditions.

In order to achieve optimal analytical performance, the effects of the concentration of anchor strands (AS), $DNA_{(AgNCs)}$ and Exo III, as well as the cleavage time and temperature on the response of the biosensor were thoroughly investigated.

As the signal probe (AgNCs) is immobilized on the surface of the MBs by hybridization with the AS, the concentration of AS is a key factor that affecting the density of AgNCs on the surface of MBs. In order to optimize the concentration of AS used in the preparation step of AgNCs-MBs, FAM was labeled at the 3' end of AS and conjugated with COOH-MBs at different concentrations. As shown in Figure 2A, the fluorescence intensity of FAM at 517 nm increases notably with an increasing concentration of FAM-AS and reaches a plateau when the concentration is about 7 μM. Thus, 7 μM was selected as the optimal AS concentration. As signal probe, the concentration of $DNA_{(AgNCs)}$ is another important parameter affecting the biosensor performance. In this system, the density of DNA@AgNCs immobilized on the surface of MBs was optimized by optimizing the concentration of $DNA_{(AgNCs)}$ from 0.05 to 5.3 μM. As shown in Figure 2B, the fluorescence intensity of AgNCs at 641nm increases with the increase of the concentration of $DNA_{(AgNCs)}$ and reaches a plateau when the concentration exceeds 2.0 μM. Therefore, the concentration of 2.0 μM was used in this experiment.

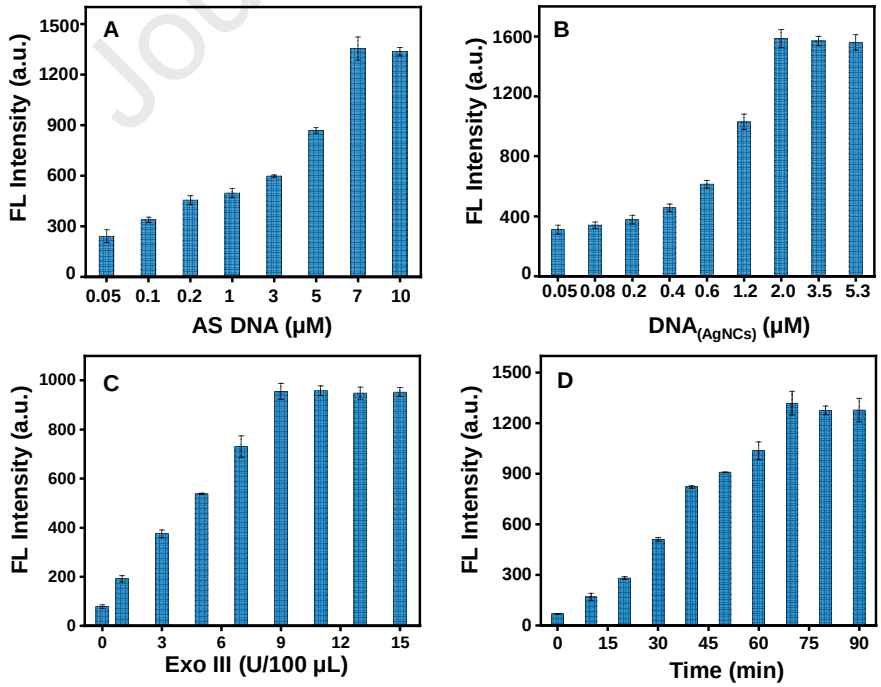

Figure 2. The effect of (A) concentration of AS DNA, (B) concentration of $DNA_{(AgNCs)}$, (C) concentration of Exo III and (D) cleavage time on the performance of the biosensor. p53

concentration: 1 pM; For A: FAM labeled AS DNA was used instead of AS DNA, and the fluorescence intensity of FAM at 517 nm was measured with λ_{ex}= 480 nm; for B-D: the fluorescence intensity of AgNCs at 641 nm was measured with λ_{ex}=528 nm.

Exo III is the driving force for this cascade amplification system, thus its concentration affects the performance of the biosensor. Figure 2C reveals that as the concentration of Exo III increases from 0 to 15 U/100 μL, the fluorescence response gradually increases and reaches a maximum when the Exo III concentration is about 9 U/100 μL. As both ERA and walking is powered by Exo III, the two amplification steps can be integrated into one-step, i.e., one-pot homogeneous amplification reaction was adopted. Sufficient digestion time ensures maximum signal amplification. As can be seen in Figure 2D, the fluorescence intensity increases along with the digestion time and reaches plateau at 70 min. Thus, the optimal digestion time was chosen at 70 min. Enzyme activity limits the reaction rate of the biosensing system [28], and the temperature is an important factor affecting enzyme activity. Therefore, the reaction temperature was also optimized and the results are shown in Figure S3. When reacted at 37 °C, the biosensor performs the best. Therefore, 37 °C was chosen as the reaction temperature. In summary, the biosensor is constructed by conjugating MBs with AS DNA (7 μM) and $DNA_{(AgNCs)}$ (2.0 μM); the cascade amplification system of ERA and DNA walker is proceeded at 37 °C, with Exo III concentration of 9 U/100 μL for 70 min.

3.4 Analytical performance and practical application.

Under optimized conditions, the sensitivity of the proposed biosensor was evaluated by adding different concentrations of p53 in the range of 0 to 1 pM. As shown in Figure 3, the fluorescence intensity exhibits a good linear correlation with the logarithm of the concentration of p53 in the range of 40-1000 fM with a correlation coefficient of 0.9848. The fitting equation is F= 509.6 log C_{p53}-327. Based

on the equation $C_{LOD} = 3S/k$ (where k is defined as the slope of regression equation, C_{LOD} refers to the limit of detection (LOD), and *S* refers to the standard deviation of the blank (N =9)), the LOD is calculated to be 18 fM. This detection limit is lower or comparable to previously reported methods for gene detection (Table 1). Although ERA-based signal amplification methods have previously been reported for the sensitive detection of gene, our ERA+DNA walker approach employs one type of enzyme in both ERA and walking, which facilitates one-pot detection and largely simplifies the operation procedure. Besides, instead of using fluorophore labeled DNA strands, fluorescent AgNCs were synthesized using DNA strands as template, facilitating sensitive cascade amplification detection of nucleic acid analytes at relatively low cost.

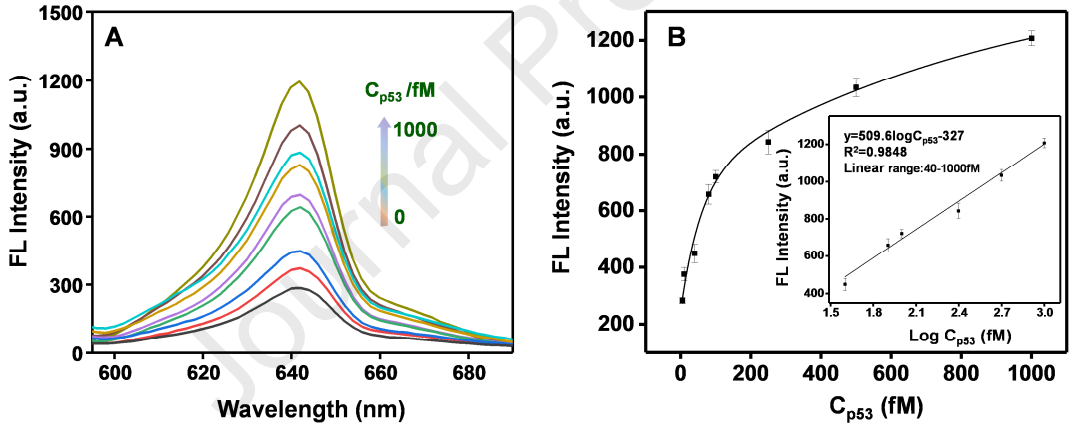

Figure 3. (A) Fluorescence spectra of the biosensor in the presence of various concentrations of p53 (0-1000 fM). (B) Calibration curve corresponding to the fluorescence signals with different concentrations of p53. Inset: Linear calibration curve between fluorescence intensity and the logarithm of p53 concentration within a range of 40-1000 fM. For (B), the fluorescence intensity of AgNCs at 641 nm was recorded with λ_{ex}= 528 nm;

Table 1. Comparison of different amplification methods for nucleic acid detection.

Target	Amplification strategy	Detection method	Detection range	Detection limit	Ref.
DNA	CHA	colorimetric	20 -1 ×10^3 pM	20 pM	15
DNA	Exo III-assisted target recycling amplification	fluorescent	0.1 -1 pM	0.52 pM	16
miRNA	DNA walker + RCA	fluorescent	0.1 -1 ×10^3 pM	0.58 pM	17
miRNA	DNase I-assisted target recycling	fluorescent	10 -1 ×10^3 pM	2.3 pM	18
antibiotics	Nt.BbvCI-assisted nicking cyclic+ Exo III-aided cyclic amplification	electrochemistry	0.1 -1 ×10^3 pM	0.83 pM	19
DNA	Exo III-assisted target recycling +CHA	electrochemistry	0.1 -5 ×10^3 pM	0.92 pM	20
DNA	Exo III-assisted target recycling + 3D DNA walker	fluorescent	0.40 -1 pM	0.18 pM	This work

High specificity is a necessary property of biosensor. Therefore, the specificity of the biosensor was also investigated by measuring the response of four kinds of DNA counterparts, including target DNA (p53), single-base mismatched DNA (M-1, M-2), two-base mismatched DNA (M-3, M-4), three-base mismatched DNA (M-5, M-6) and randomly mismatched sequence (MS) at the same concentration. As shown in Figure 4, an obvious fluorescence signal was observed in response to the target, and the fluorescence signal of the target was about 1.94 times, 2.06 times, 2.45 times, 3.34 times, 5.67 times, 6.15 times, 8.65 times, 15.9 times as that of M-1, M-2, M-3 M-4, M-5, M-6, MS and Blank, respectively. As shown in Figure S4, the biosensor also has certain specific recognition ability in different sample matrix including human serum and urine. These results all indicate that the ERA and DNA walker-based cascade amplification biosensor enables specific detection of p53.

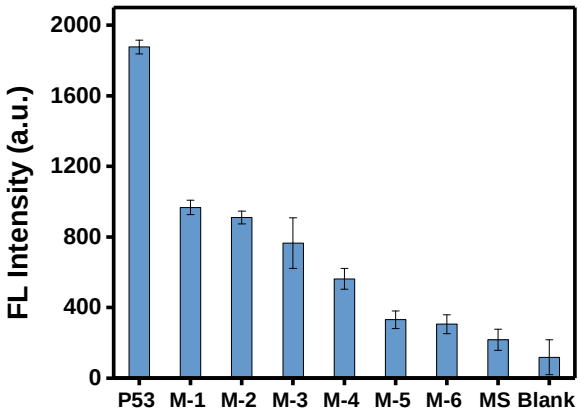

Figure 4. Specificity investigation of the biosensor for p53 detection. The fluorescence intensity of AgNCs at 641 nm was recorded with λ_{ex}= 528 nm; error bars are the standard deviations taken from three independent experiments. p53 and mismatch DNA concentration: 1pM.

To explore the potential application in biological sample, the biosensor was employed to detect p53 in human serum and urine samples. As the level of p53 in serum from a healthy volunteer was low and not detectable with our approach, different concentrations of p53 were spiked into serum samples for the evaluation of recoveries. According to the analysis results of sample 1~ 4 in Table S2, the recovery of the p53 analysis was ranging from 96% to 108% along with relative standard deviation (RSD) of 2.1-5.1%. The analysis results of urine samples 1~ 3 are shown in Table S3, with the recoveries ranging from 94% to 103% and the RSD within 2.3-6.2%. These results suggested that the proposed biosensor holds the practical potential in the detection of cancer-related single-stranded DNA fragment. It should be pointed out that the suitable analyte of this biosensor is short single-stranded DNA, whereas the cancer-related gene exists in the form of double-stranded DNA in human serums. Therefore, for the application of this biosensor in cancer diagnosis, DNA extraction from clinical samples and PCR amplification step are required to get single-stranded cancer-related gene copies for further quantification.

4. Conclusion

In conclusion, a simple, one-pot and ultrasensitive isothermal cascade amplification strategy was proposed for the construction of highly sensitive and

selective DNA sensor. This DNA sensor has several advantages. First, one-step reaction avoids complicated operation procedure thus facilitates simple and fast nucleic acid detection. Second, compared with amplification cascade driven by multiple enzymes, the single-enzyme driven cascade amplification is simpler and cheaper. Meanwhile, it is also more efficient with respect to enzyme-free system.

Under optimal conditions, this biosensor showed high sensitivity and specificity for p53 detection with the LOD down to 18 fM. Moreover, it could be expanded easily to other targets by simply changing the recognition sequence of the hairpin probe. Thus, this new methodology can be expected to provide a highly sensitive platform for the amplified analysis of various target molecules.

ASSOCIATED CONTENT

*Supporting Information

Oligonucleotides sequences of DNA used in this work; SEM, EDS spectrum and confocal fluorescent microscope images of MBs and AgNCs-MBs; The effect of temperature on the performance of the biosensor; Specificity of the biosensor in other sample matrix. Analysis results of real samples.

AUTHOR INFORMATION

*Corresponding author.

E-mail address: yangting@mail.neu.edu.cn (T. Yang).

Tel: +86 24 83688944; Fax: +86 24 83676698

Conflicts of interest

The authors declare that they have no known competing financial interests or personal relationships that could have appeared to influence the work reported in this paper.

ACKNOWLEDGEMENTS

Financial support from the Natural Science Foundation of China (21874014,

21727811, 21675019), the Fundamental Research Funds for the Central Universities (N180505021, N170506004, N2005017, N2005027) are highly appreciated. Special thanks are due to the instrumental analysis from the equipment share and collaboration platform in the department of chemistry, Northeastern University.

ETHICAL STATEMENT

All experiments involving human serum samples and urine samples are performed in compliance with the relevant laws and institutional guidelines and have been approved by the ethical committee of Northeastern University, China.

REFERENCES

[1] T. Miyashita, J. C. Reed, Tumor suppressor p53 is a direct transcriptional activator of the human bax gene, Cell. 80 (1995) 293-299.

[2] M. Hasazadeh, N. Shadjou, M. de. La. Guardia, Current advancement in immuosensing of p53 tumor suppressor protein based on nanomaterials: analytical approach, Trac. Trend. Anal. Chem. 89 (2017) 13-20.

[3] Xu. J. G, Wu. Z. S, Wang. Z. M, Li. H. L, Le. J. Q, Lee. J. Two-wheel drive-based DNA nanomachine and its sensing potential for highly sensitive analysis of cancer-related gene, Biomaterials. 100 (2016) 110-117.

[4] Zhao. Y. X, Chen. F, Li. Q, Wang. L. H, Fan. C. H, Isothermal amplification of nucleic acids, Chem. Rev. 115 (2015) 12491-545.

[5] Jung. C, Ellington. A. D, Diagnostic applications of nucleic acid circuits, Acc. Chem. Res. 47 (2014) 1825-35.

[6] Deng. R. J, Zhang. K. X, Li. J. H, Isothermal amplification for microRNA detection: from the test tube to the cell, Acc. Chem. Res. 50 (2017) 1059-1068.

[7] Zheng. J, Ji. X. H, Du. M. Y, Tian. S. B, He. Z. K, Rational construction of a DNA nanomachine for HIV nucleic acid ultrasensitive sensing, Nanoscale. 10 (2018) 17206-17211.

[8] Bi. S, Li. L, Zhang. S. S, Triggered polycatenated DNA scaffolds for DNA sensors and aptasensor by a combination of rolling circle amplification and

DNAzyme amplification. Anal. Chem. 82 (2010) 9447-9454.

[9] Qin. P. Z, Yao. L, Xu. J.G, Liu. G. D, Chen. W, Smart engineering of a dual-DNA machine with a high signal-to-noise ratio for one-pot robust and sensitive MiRNA signaling, Chem. Commun. 55 (2019) 14367-14370.

[10] Wang. L. J, Zhang. Y, Zhang. C.Y, A target-triggered exponential amplification-based DNAzyme biosensor for ultrasensitive detection of folate receptors, Chem. Commun. 50 (2014) 15393-15396.

[11] Cheglakov. Z, Weizmann. Y, Basnar. B, Willner. I, Diagnosing viruses by the rolling circle amplified synthesis of DNAzymes, Org. Biomol. Chem. 5 (2007) 223-225.

[12] Quan. K, Huang. J, Yang. X. H, Yang. Y. J, Ying. L, Wang. H, Xie. N. L, Ou. M, Wang. K. M, Powerful amplification cascades of FRET-based two-layer nonenzymatic nucleic acid circuits, Anal. Chem. 88 (2016) 5857-64.

[13] Liu. L, Liu. J. W, Wu.H, Wang. X. N, Yu. R. Q, Jiang. J. H, Branched hybridization chain reaction circuit for ultrasensitive localizable imaging of mRNA in living cells, Anal.Chem. 90 (2018) 1502-1505.

[14] Li. W, Wang. L, Jiang. W, A catalytic assembled enzyme-free three-dimensional DNA walker and its sensing application, Chem. Commun. 53 (2017) 5527-5530.

[15] Zheng. A. X, Li. J, Wang. J. R, Song. X. R, Chen. G. N, Y. H. H, Enzyme-free signal amplification in the DNAzyme sensor via Target-Catalyzed Hairpin Assembly, Chem.Comm. 48 (2012) 3112-3114.

[16] Wang. K, Zhai. F. H, He. M. Q, Wang. J, Yu. Y. L, He. R. H, A simple enzyme-assisted cascade amplification strategy for ultrasensitive and label-free detection of DNA, Anal. Bioanal. Chem. 441 (2018) 4569-4576.

[17] Wang.L.D, Deng. R. J, Li. J. H, Target-fueled DNA walker for highly selective miRNA detection, Chem. Sci. 6 (2015) 6777-6782.

[18] Xie. Y, Lin. X. Y, Huang. Y. S, Pan. R. J, Zhu. Z, Zhou. L. J, Yang. C.Y. J, Highly sensitive and selective detection of miRNA:DNase I-assisted target recycling using DNA probes protected by polydopamine nanospheres, Chem. Comm. 51 (2015) 2156-2158.

[19] Zhang. R. F, Wang. Y, Qu. X. N, Li. S. S, Zhao. Y. H, Zhang. F. F, Liu. S, Huang. J. D, Yu. J. H, A label-free electrochemical platform for the detection of antibiotics based on cascade enzymatic amplification coupled with a split G-quadruplex DNAzyme, Analyst. 144 (2019) 4995-5002.

[20] Tao. C. Y, Yan. Y. R, Xiang. H, Zhu. D, Cheng. W, Ju. H. X, Ding. S. J, A new mode for highly sensitive and specific detection of DNA based on exonuclease III-assisted target recycling amplification and mismatched catalytic hairpin assembly, Chem. Comm. 51 (2015) 4220-4222.

[21] Gao. Y, Li. B. X, Exonulese III-assisted cascade signal amplifiation strategy for label-free and ultrasensitive chemluminesence detection of DNA, Anal.Chem. 17 (2014) 8881-8887.

[22] Pei. Q. Q, Wang. Y, Liu. S, Qin. Y. F, Leng. X. Q, Cui.X. J, Huang. J. D, Exonuclease III-aided autonomous cascade signal amplification: a facile and universal DNA biosensing platform for ultrasensitive electrochemical detection of S. typhimurium, New. J. Chem. 41 (2017) 7613-7620.

[23] Zhang. K. Y, Yang. L, Lu. F, Wu. X. C, Zhu. J. J, A universal upconversion sensing platform for the sensitive detection of tumour-related ncRNA through an Exo III-assisted cycling amplification strategy, Small. 14 (2018) 1703858.

[24] Wang. Z. H, Xia. J. F, Song. D. M, Zhang. F. F, Yang. M, Gui. R. J, Xia. L, Bi. S, Xia. Y. Z, Lable-free quadruple signal amplification strategy for sensitive electrochemical p53 gene biosensing, Biosens. Bioelectron. 77 (2016) 157-163.

[25] Liu. L, Lu. H, Shi. R. X, Peng. X. X, Xiang. Q. W, Wang. B. W, Wan. Q. Q, Sun. Y. J, Yang. F, Zhang. G. J, Synergy of peptide-nucleic acid and spherical nucleic acid enabled quantitative and specific detection of tumor exosomal microRNA, Anal. Chem. 91 (2019) 13198-13205.

[26] Chen. J, Luo. Z. W, Sun. C. J, Huang. Z. J, Zhou. C, Yin. S, Duan. Y. X, Li. Y. X, Research progress of DNA walker and its recent applications in biosensor, Trac. Trend. Anal. Chem. 120 (2019) 115626.

[27] He. F, Ye. Z. Y, Zhao. L. D, Yin. B. C, Ye. B. C, Probing exosome internalization pathways through confocal microscopy imaging, Chem. Commun. 93 (2019)

14015-14018.

[28] Zhou. X. L, Xia. F, Guo. Xiao. Y, Kevin. W. Plaxco, Sensitive and selective amplified fluorescence DNA detection based on exonuclease III-aided target recycling. J. Am. Chem. Soc. 132 (2010) 1816-1818.

[29] He. M. Q, Wang. K, Wang. W. J, Yu. Y. L, Wang. J. H, Smart DNA machine for carcinoembryonic antigen detection by exonuclease III-assisted target recycling and DNA walker cascade amplification, Anal. Chem. 89 (2017) 9292-9298.

[30] Wang. R, Wang. L, Xua. X. W, Jiang, W, An enzyme-free and label-free fluorescence biosensor for microRNA detection based on cascade amplification of DNAzyme-powered three-dimensional DNA walker and hybridization chain reaction, Sens. Actuators B Chem. 268 (2018) 287-292.

[31] Zhou. W. J, Zhou. J. B, Teng. Y, Du. B. J, Han. X, Dong. S. J, Novel dual fluorescence temperature-sensitive chameleon DNA-templated silver nanocluster pair for intracellular thermometry, Nano Res. 11 (2018) 2012-2023.

Highlight

- An Exo III-assisted target recycling amplification (ERA) and 3D DNA walker cascade amplification system was constructed.
- Two-step amplification was integrated into one-pot cascade amplification which is much simpler in operation.

Declaration of interests

The authors declare that they have no known competing financial interests or personal relationships that could have appeared to influence the work reported in this paper.